Chapter 1

INTRODUCTION

AND

LITERATURE REVIEW

CHAPTER - 1

INTRODUCTION AND LITERATURE REVIEW

1.1 INTRODUCTION

This chapter describes current status of the materials used in biomass fired power plants and the associated problems. It also provides details of physical metallurgy, mechanical properties, oxidation and hot corrosion behavior of the 904L super austenitic stainless steel (SASS) and its comparison with the other SASS grades.

Worldwide, consumption of electricity is an important requirement of the industries and society. Majority of the electricity production units are dependent on conventional sources of fuels such as coal and gas. Conventional grades of fuels such as coal/coke emit harmful gases CO_2 and SO_2 which are responsible for global warming. To tackle these environmental issues, researchers advised government and private industries to focus on the key aspects of using non-conventional grades of fuels to fulfil the growing demand of power consumption. It was suggested that solid wastes generated from different sources such as domestic and industries, could be an excellent means of energy. In future, solid wastes can share coal along with other sources of fuel [1, 2].

Solid wastes are easily available in form of agriculture, municipal garbage, industrial and other domestic wastes. The daily generation of these wastes is more than 1000 tons per day. There are three categories of conventional methods to tackle these solid wastes: 1. Recycling, 2. Combusting and 3. Land fillings. Recycling is possible but it's a costliest as well as infeasible for re-use every time. Combustion is one of the easiest mode by which

solid wastes can be minimized, however, it simultaneously gives rise to air pollution. Land filling is also possible but attributes to contamination of earth crust as well as underground water. Solid wastes combustion, if applied in a proper way, can solve the issues of a global scenario. Developed countries like USA, China, UK, Japan, Germany, France, Sweden and others have contributed to this ideal solution to control pollution by building and managing power plants, using solid wastes instead of conventional fuels [3]. It is remarkable achievement that a developing country like India had initiated building power units based on non-conventional fuel consumption, like biomass solid waste.

Metallurgical Problems

Yet, the problem is not at an end, another problem is related to metallurgical failure occurring over the surfaces of super heater tubes during combustion of fuel/charge in coal as well as biomass fuel fired based power stations. Service life of super heater tubes, when subjected to fuel combustion is severely affected by ash deposition. A large number of metals and alloys are used in such power plants. A list of common super heater materials used for biomass combustion is given in **Table 1.1**.

Several investigations concluded that solid waste, also called as biomass, when used for combustion, give rise to generation/segregation of ash deposition of very complex chemistry [4]. Moreover, due to these depositions, the heat transfer through super heaters to boiler chamber becomes 50% less efficient in biomass fuels than that of coal-fired fuels. The biomass ash deposits are more complex than the chemistry generated by coal combustion. Alkali chlorides are found to be dominant, which form low melting eutectics with surface oxides of the super heater tube surface and react in such a way that service life

of the component is reduced and followed by frequent shut downs and thinning of the wall surface [5].

1.1.1 SUPER AUSTENITIC STAINLESS STEEL (SASS)

1.1.1.1 HISTORICAL DEVELOPMENTS

The conceptual name of super austenitic stainless steels comes from super ferritic and super duplex stainless steels [6]. SASS grades are sub-group of austenitic stainless steels containing high amounts of Mo, Ni and to some extent nitrogen. The composition of these steels are presented in **Tables 1.1**.

These materials are also known as Fe-Ni-Cr alloys, possessing austenitic microstructure. These alloys have been developed for industries with harsh conditions [7]. To cope with austenitic inter granular corrosion susceptibility after welding, Ti and Ta were added as carbide stabilizing elements, earlier. With advent of Argon Oxygen Decarburization (**AOD)** and Vacuum Oxygen Decarburizing (VOD) refining techniques in 1960s, carbon content in the SS was reduced to less than 0.03%, which solved the problem of intergranular corrosion susceptibility. As a result, in 1980s, new ASS was developed having ultra low carbon content. Moreover, with increased Cr, Ni and Mo, along with addition of Mn, Cu, Si in 304L and 316L SS grades, new highly alloyed grades such as 317LM (4.5% Mo), 904L, 316L (Urea grade), 347 (nitric acid grade), 348 (nuclear grade) were produced.

Later, development in 1970s took place by addition of N and B to enhance the properties of SASS grades such as AL-6XN, alloy 926. Among all the grades of stainless steel, SASS has more demand for technical applications in industries and possible

3

replacements of ASS, and a substitute to Ni-base super alloys. SASS grades are hard to melt, also easily segregate and crack. Most common property of these grades is that they can be cold worked and hot worked. Common applications of these SASS grades are listed in **Table 1.2**.

Table 1.1: Chemical compositions of super austenitic stainless steels. [8-11]

Alloy	C	Mn	P	S	Si	Cr	Ni	Mo	Cu	Fe	N
Chemical Composition (wt %)											
904L	≤ 0.02	≤ 2	$\leq$ 0.045	$\leq$ 0.035	≤ 1	19 ~ 23	23 ~ 28	4 ~ 5	1 ~ 2	Bal	$\leq$ 0.10
254SMo	≤ 0.02	≤ 1	≤ 0.03	$\leq$ 0.01	≤ 0.8	19.5 ~ 20.5	17.5 ~ 18.5	6 ~ 6.5	0.5 ~ 1	Bal	0.18 ~ 0.22
654SMo	≤ 0.02	2 ~ 4	≤ 0.03	$\leq$ 0.005	≤ 0.5	24 ~ 25	21 ~ 23	7 ~ 8	0.3 ~ 0.6	Bal	0.45 ~ 0.55
Incoloy 926	≤ 0.02	≤ 2	≤ 0.03	$\leq$ 0.01	≤ 0.5	19 ~ 21	24 ~ 26	6 ~ 7	0.5 ~ 1.5	bal	0.15 ~ 0.25

Table 1.2: Application of super austenitic stainless steel.

Area	Applications
Ocean	Marine structures in the sea shore environment, desalination of seawater, marine aquaculture, seawater heat exchange, etc.
Environmental Protection	Flue gas desulphurization device used in thermal power generation, wastewater treatment technique, etc.
Petrochemical Industry	Refining process, chemical equipment
Energy	Power generation, comprehensive utilization of coal, and ocean wave power generation.;
Food	Salt making equipments, etc.

1.1.1.2 904L SASS

SASS 904L was originally developed by the French company, named H.S. It contains less amount of carbon but high Cr, Ni and Mo. It possesses relevant property of activation and passivation conversion ability. It has very high corrosion resistance, particularly in sulphuric acid, formic acid, phosphoric acid and acetic acid, the non-oxidizing acids. It possesses high resistance against pitting in neutral chloride containing media, crevice as well as stress corrosion cracking. It can sustain H_2SO_4 of different concentrations below 70 ˚C. This steel is corrosion resistant in acetic acid and also in mixture of formic acid and acetic acid over a wide range of temperature at normal pressure. This steel is austenitic and resistant to ferrite and α-phase precipitation.

The high nickel content in this steel reduces the effects of corrosion active sites during exposure in reducing atmosphere like sulphuric and formic acids and also lowers the rate of corrosion from the sites like pits and gaps. 904L possesses very high resistance against corrosion in pure form of phosphoric acid over a wide range of concentration up to 85%. Thus, when industrial phosphoric acid is prepared through wet processing, the impurities produced could be easily sustained by 904L, without affecting its corrosion resistance.

During an exposure to highly oxidizing nitric acid solution, it survives mildly with much better corrosion resistance compared to highly alloyed steel. However, its application under exposure of hydrochloric acid is restricted to very low concentration (1-2%), in this range of concentration, this steel exhibits corrosion resistance superior to those of other common stainless steels.

904L SASS exhibits high resistance against pitting corrosion, also its resistance to crevice corrosion in chloride containing solutions is comparatively better than those of traditional stainless steels, above 60 °C. Due to its high nickel content, 904L is highly resistant to stress corrosion cracking in the solutions containing chloride, concentrated hydroxide and in the environment rich in hydrogen sulphide.

In this thesis, oxidation and hot corrosion behavior of the 904L super austenitic stainless steel, at elevated temperatures, is presented. Some important data on tensile properties of this steel from 20-500 °C are displayed in **Table 1.3**.

Table 1.3: Tensile properties of 904L SASS at elevated temperature [10]

°C	$R_p0.2$	$R_p0.1$	R_m	Y.S 0.2%	Y.S 0.1%	UTS	Elongation
	MPa			Ksi			%
20	313	275	520	45	39	75	40
100	205	230	520	30	33	75	40
300	145	170	490	21	26	71	40
500	125	150	410	18	22	35	40

1.2 LITERATURE REVIEW

1.2.1 OXIDATION OF SASS

This section deals with the interesting facts on the oxidation behavior of sub group of SASS such as Sanicro-25 & 28, SMO-654, SMO-254 and others under varying atmospheres.

Scales formed during oxidation of SASS (Fe-Ni-Cr alloy) with more than 20wt% Cr, consist of inner layer of Cr_2O_3 and a layer of spinel over it [12-14]. Increase in ratio of

Ni/Fe causes decrease in activity of iron and hence its solubility in Cr_2O_3 is minimized which consequently affects formation of spinel. Thus, heat resisting steels often consist of 10-20wt% Ni and have austenite matrix. At higher levels of Ni, protection against formation of Fe spinel can be achieved. Later, steel grades were formulated on the basis of Fe-(10-20)Ni and Ni-(20-26)Cr, which are extensively used over the temperature range from 900-1100 ˚C, depending upon the environment.

Li et.al. [15] investigated oxidation behavior of S32654 over the temperature range from 900-1200 ˚C under air and showed that there was catastrophic oxidation and parabolic rate law was followed up to 10 h of exposure, whereas exposures above 10 h, the trend changed and linear rate law was followed at 900 ˚C. It was reported that during the initial exposure up to 10 h parabolic rate law was due to formation of $MnMoO_4$ molybdate from electrochemical reaction which acted as a barrier to anionic and cationic diffusion, whereas for more than 10 h the rate becomes linear due to formation of molten $MnMoO_4$-MoO_3 molybdate which promoted cracking over the oxidized layer. Formation of MoO_3 leads to development of pores and cracks. Nitrogen in the alloy induces Cr_2N precipitation, which reduces the tendency of formation of Cr-rich layer and also promotes rapid transport of transmission channels for Mo, Mn, N and O, which enhances the oxidation phenomenon.

Earlier studies on Mo by Gulbransen et.al. [16] suggested that during oxidation of Mo below 450 ˚C the oxide layer was adherent, whereas during exposure at 500-700 ˚C the oxide scale becomes volatile, which is probably due to chemical type of reaction between the scale and metal interface. Also, it was suggested that above 801 ˚C the volatility of Mo increased due to high active chemical process on the metal surface which resulted in faster

7

evaporation of MoO_3. There exist two forms of volatile oxides of Mo, MoO_2 and MoO_3. MoO_2 is stable above 800 ˚C, whereas MoO_3 continuously volatilizes or reduced at all the temperatures.

Intiso et al. [17] conducted isothermal oxidation test, from 600-750 ˚C under dry and wet environments on Sanicro-25. This study showed that in temperature range of 600-750 ˚C under dry O_2, the alloy forms a uniform thin protective layer whereas, under wet environment the scale remains protective up to 600 ˚C. At 700 and 750 ˚C the alloy suffers from breakaway, due to volatilization of chromic acid which depletes the chromium from substrate. Similar type of isothermal oxidation tests was performed by C. Peterson and co-workers [18] on Sanicro-28 but at 700, 800 and 900 ˚C in dry and wet environment. They reported that Sanicro-28 under both the environments forms protective scale. The scale was duplex type. The inner layer was corundum type oxide $(Fe, Cr)_2O_3$ and the outer layer consisted of a spinel.

Rutkowski et al. [19] investigated the oxidation process of Sanicro-25 under steam at 700 ˚C for a prolonged exposure up to 5000 h and observed Cr_2O_3 at the scale whereas beneath the scale, Cr-depleted zone was evolved. In the other areas which were not affected by oxidation, precipitates of $M_{23}C_6$, ε-Cu and some Laves phases were reported.

Zhu et al. [20] conducted isothermal oxidation test on Sanicro-25 and TP347HFG under super critical water (SCW) at 600, 650 and 750 ˚C for up to 1000 h. They showed that, weight change in the case of TP347HFG was higher than that in Sanicro-25. Also, the amount of chromium oxide formed in TP347HFG was higher in Sanicro-25. The layer was uniform at 600-700 ˚C.

In case of SASS, most of the studies were carried out over the temperature range of 450-700 °C under flowing air as well as in humid air atmosphere that the application of SASS at elevated temperatures such as 700-1000 °C may promote precipitation of intermetallic phases as well as volatilization of important oxides. Yanhui et.al. [21] suggested that early stage of oxidation can be categorized into 3 stages. 1-Rapid oxidation; 2-Transitory and 3-Diffusion controlled, due to increase in temperature of oxidation. During initial stage at higher temperature, rapid growth of Fe/Cr oxides such as Cr_2O_3, Fe_2O_3 and Fe_3O_4 dominates the oxide layered enrichment followed by transient stage, where Cr preferentially enriches at the inner layer by lateral linkage of Cr oxide spinels and the outward transport of Fe rich oxide; further oxidation continues by obstructing behavior of inner spinels promoting barrier to the later stages of Fe to diffuse at the surface region and slows down the diffusion process. Thus, under SCW environment, mechanism of oxide growth arises by species Cr^{6+} and promotes the formation of $CrO_2(OH)_2$ which takes birth in very early stages, up to 40 h of exposure at 465-580 °C, during which formation of Fe_2O_3 is inhibited and forced to form Fe_3O_4.

1.2.2 HOT CORROSION OF SASS DURING BIOMASS COMBUSTION

This section deals with brief details of corrosion of SASS due to deposit of ashes during biomass combustions. As stated earlier, utilization of biomass as solid fuel, results in initial corrosion of the metal surface at ≈400 °C and further rises to 500 °C slowly. Just above 500 °C, the rate of corrosion increases rapidly, which is not acceptable as well as it may result in shortening of service life of the heater tubes. From the chemical analysis of the ash deposits formed from biomass combustion, it was found that the concentration of the

harmful salts such as of Na, K, Cl and S and other heavy elements such as Pb, Zn and Ca, deteriorates the property of heater tubes. From the literature it was found that K was mainly present in higher proportion in the biomass ash deposit in the form of KCl and K_2SO_4, which is found to be normally low in the coal ash deposits. Several researchers investigated the effect of KCl and K_2SO_4 and found that in the absence of KCl in the ash deposits, the rate of corrosion was very low, whereas in presence of $KCl+K_2SO_4$ slight increase in the rate of corrosion was observed. Many studies suggested that presence of K_2SO_4 may provide beneficial effect for protection of tubing materials.

The effects of sulphates and chlorides on hot corrosion of boiler tube materials such as Inconel 625, T22, 310H, 347H, Sanicro-28 and Esshete 1250, at temperature of 500 ˚C for 500 h, was studied by Liu et al. [22]. In general, while testing these tube materials under simulated WTE type environment at 500 ˚C, a trend of increasing corrosivity was observed as $CaCl_2<NaCl<KCl<ZnCl_2<PbCl_2<FeCl_2$. They proposed mechanisms of chloride to corrode the material through vicious cycles, in which a shorter path of the cycle leads to a higher rate of corrosion. In their investigation, $FeCl_2$ was found to follow shortest path towards corrosivity, associated with higher rate of corrosion. Moreover, highly alloyed material Inconel 625, suffered significant wall thinning during fireside corrosion of super heater tubes, while from exposures in metal chlorides Sanicro-28, 347H and Esshete 1250 suffered from grain boundary deterioration. It was suggested that sulphates of Pb and Zn are less corrosive than their chlorides. Chlorides have high volatile ability and far higher ability on upgrading the rates of corrosion of the tube materials. Thus, chlorides are more effective at 500 ˚C than sulphates in the waste fired boilers. During long exposures up to 500 h, it was found that Esshete 1250 and T22 showed weak

10

corrosion resistance to chlorides of Zn and Pb containing salts. In comparison of all the studied materials Inconel 625 showed better performance. The kinetic studies revealed that Sanicro-28, T22 and Esshete 1250 showed comparable performance in short term exposures. However, a trend of increasing thickness during corrosion of the boiler material was proposed as Sanicro-28<Esshete 1250<T22. Moreover, their study revealed that Ni/Cr ratio played significant role in decreasing corrosion kinetics of T22, Esshete 1250 and Sanicro-28.

Enestam et al. [23] examined severity of corrosion due to KCl and NaCl on alloys 10CrMo9-10, AISI 347 and Sanicro-28 at 400-650 ˚C in air. The corrosive action of both the salts was significantly high at higher temperature. A mechanism was proposed, associated with both, vaporization of metal chlorides as well as oxidation of chlorides. The AISI 347 unveiled initial sign of corrosion at 500 ˚C due to high tendency of volatilization of metal chlorides, whereas no sign of corrosion was revealed up to 475 ˚C in the Sanicro-28. Corrosion of Sanicro-28 occurred at 600-650 ˚C from exposure in the salt environment of NaCl as well as KCl. There were more internal losses in NaCl, on the other hand the amounts of corrosion products/oxides were more in the KCl environment. The internal damage might have been due to larger grain size which is known to limit/slowdown the healing property of the protective chromium. It was observed from this study that the extent of oxidation was higher from exposure in NaCl than that in KCl on the AISI 347 as well as on 10CrMo9-10. It is clearly revealed from this study that difference in the content of alloying elements (Fe, Ni and Cr) may not be affecting only the rates of corrosion but also differs from the general concept that enrichment of Cr in the alloy can provide higher resistance to oxidation.

11

A similar study on corrosivity of salts NaCl and KCl was conducted by Makippa et al. [24] on Sanicro-25 for short duration of 35h. It was observed that alloys with high content of Cr were affected less by NaCl than by KCl.

The observation made by Makippa et al. [24] was supported by Lehmusta et al. [25]. They showed that both NaCl as well as KCl activates/increases or cause selective oxidation of metallic chromium. They also proposed, in contrast to the earlier statements [23], that the rate of oxidation of Cr in the presence of KCl, is much higher than that from the exposure in NaCl environment in temperature range of 550-600 ˚C.

Proff et al. [26] showed that, high temperature corrosion of SASS, under flue gas evironment accelerates the rate of corrosion of boiler material. This is due to the rich contents of water vapor and alkali salts in flue gases. Sanicro-28, a highly alloyed austenitic stainless steel when subjected to KCl solid particles under the laboratory exposures at 600 ˚C for 1-168 h in $5\%O_2 + 40\%H_2O$ led to breakdown of protective film [26, 27]. During the experiments KCl particles were coated up to 0.10 mg/cm^2. Charaterization of the corroded samples, revealed complex chemistry of corrosives, mainly of K_2CrO_4 and the rapid transport of iron species on the surface resulted in accumulation of oxide on the former KCl particles. The consumption of chromium and the presence of chloride on the surface does not result in breakdown of the protective oxide. The high ability of the alloy to withstand the severe environment is attributed to the high ratio of Cr/Fe. Longer duration exposure up to 168 h, was found not to cause significant change in morphology in respect of that resulting from the exposure of 24 h. Thus, initial exposure of KCl salts may not promote breakaway whereas multiple deposition cycles of salts particles may lead to breakaway oxidation.

Alloy Sanicro-28 formed a thin layer of protective iron-chromium oxide [28], on the exposure to humid air at 600 ˚C. The protective oxide has been reported to react in the presence of KCl to form potassium chromate [29] as per following reaction as:

$$46KCl_{(s)} + (Cr_xFe_{1-x})_2O_{3(s)} + 1.5O_2(g) + 26H_2O_{(g)} \rightarrow 2K_2CrO_{4(s)} + (1-x)Fe_2O_{3(s)} + 4HCl_{(g)}$$
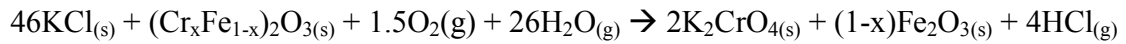
Large amount of potassium chromate was found to form and only small quantity of the potassium chloride was left. As per the above reaction, the potassium chromate should be accompanied by chromium depletion of the oxide. The austenitic stainless steel 304L also exhibited similar behavior [30, 31]. The reaction was completed after 24 h and no KCl was present on the surface. KCl is also reported to be lost by vaporization [29, 31].

Formation of heavy metal compounds during biomass combustion in WTE plants, leads to formation of eutectic mixture, which lowers the melting point of salts promoting the corrosion to occur at lower temperatures. Due to such melt down of low melting salts, corrosive gases produce an accelerated effect on corroding behavior of the molten salt. Reese and Grabke [32, 33] investigated the effect of simulated type biomass environment, by thermogravimetric experiment using solid chlorides such as NaCl, KCl, $CaCl_2$ and $MgCl_2$; on pre-oxidized samples of various alloys at 500 and 700 ˚C, under He-O_2 and He-O_2-SO_2 gaseous atmosphere. Their laboratory experiment showed that, solid-state reactions have occurred between salts and the oxide scale of the pre-oxidized sample. The main reaction products of corrosion were ferrates, chromates as well as some amount of chlorine gas. They proposed that chlorine can diffuse through cracks as well as through pores of the oxide scale towards the metal surface and react to form $FeCl_2$. Thus, it was concluded from their test that evaporation of $FeCl_2$ through the scale was rate determining step during salt induced corrosion. As mentioned earlier, $FeCl_2$ is one of the salts, which may form eutectic

melting points involving corrosion reactions to occur at lower temperatures. At 500 ˚C, vapour pressure of $FeCl_2$ reaches up to 10^{-4} bar, due to which volatilization of iron chloride occurs at faster rate and leads to diffusion through the oxide scale. This process continues and growth of iron-oxides occurs and Cl_2 gas is released. Occurence of cracks and pores in the oxide scale is detrimental for an alloy to sustain corrosion resistance. Thus, due to faster realease of Cl_2 gas and growth of iron-oxides, an unprotected metal surface is free to react with corrosive gases. This scale can also be called as non-passivating layer.

Spiegel [34, 35] studied corrosion behavior of 2.25Cr-Mo alloy using thermogravimetric setup at 500 and 600 ˚C, under simulated ash composition of KCl with heavy salts deposits such as $PbCl_2$ and $ZnCl_2$. Tests were also performed in absence of salts for testing oxidation resistance of the 2.25Cr-Mo alloy. Both the chloride salts mixtures were found to be in liquid stage at 500˚C and above. The weight gain was measured through TG experiment, at higher temperature from 500-600 ˚C, on the samples with salt deposits (such as $ZnCl_2$ and $PbCl_2$) as well as on the samples without salt deposits.
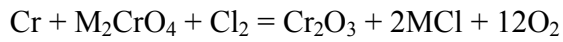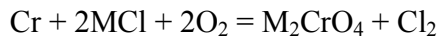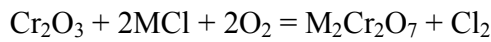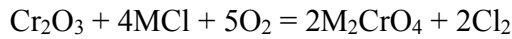
Li et al. [36] tested pure chromium for its KCl induced corrosion behavior at 650 ˚C. Their observation showed that corrosion initiated by oxidation of chromium, covered by the impression of deposited KCl salt. Tang et al. [37] investigated corrosion behavior of pure Cr, induced by NaCl environments at 500-700 ˚C and suggested that deposit of NaCl salt can significantly accelerate the corrosion in dry and wet O_2 atmosphere. It was proposed that initially Cr_2O_3 interacts with NaCl salt and reacts to form sodium chromates by releasing Cl_2 gas. Corrosion of pure Fe, Ni, Cr and its alloys was demonstrated by Li et al. [38] under $KCl-ZnCl_2$ salt environments in dry O_2 atmosphere. Though the experiments

were quite different from the actual atmosphere of waste incinerators, corrosion occurred severely even at lower temperature of 320 ˚C. TG test showed weight gain after increasing the amount of O_2 as well as salt deposits. It is noted that during their experimental study of formation of any protective oxide layer was excluded. Similar type of experiments were performed under salt mixture with 50% mol. KCl-50% mol. $ZnCl_2$, where it was revealed that pure Fe gained higher weight than that of Ni and Cr [39]. Three stages of corrosion were observed such as incubation stage, linear stage and logarithmic/parabolic stages. Thermodynamic calculation has revealed that $FeCl_2$ has higher solubility in molten KCl-$ZnCl_2$ due to formation of eutectic phases, whereas $CrCl_3$ and $NiCl_2$ possess limited solubility in molten KCl-$ZnCl_2$. Reasons behind such circumstance was pointed out that $FeCl_2$ has high outward diffusion capability than $NiCl_2$ and $CrCl_3$. Thus, higher solubility of metallic chloride leads to higher rate of diffusion with higher rate of oxidation.

Another investigation carried out on various high Cr-steels, high C-cast irons and stainless steel grade AISI 304 was under NaCl-KCL salt mixture at 670 ˚C by Vuelvas-Rayo et al. [40]. The tested samples of these grades showed weight loss, in which high C-cast iron showed highest loss in weight, followed by high Cr-steel and lowest in conventional grade of AISI 304. Thus, their study showed that C-content up to ≈4.29 (wt%) can play detrimental role during oxidation as well as corrosion process. However, their study also showed that increase in C-content above 4.29 (wt%) can minimize the rate of corrosion.

Li and Speigel [41] showed mechanism of solubility reactions between Cr_2O_3 layer and (KCl-NaCl) melts, reacts to form chromates. Thus, hot corrosion reactions forming chromate are as follows:

$Cr_2O_3 + 4MCl + 5O_2 = 2M_2CrO_4 + 2Cl_2$

$Cr_2O_3 + 2MCl + 2O_2 = M_2Cr_2O_7 + Cl_2$

$Cr + 2MCl + 2O_2 = M_2CrO_4 + Cl_2$

$Cr + M_2CrO_4 + Cl_2 = Cr_2O_3 + 2MCl + 12O_2$

In these reactions M is denoted for metallic Na or K, which combines to form chromates by releasing Cl_2 gas. Though, Cl gas acts as an oxidant, Cr can be seen to be selectively oxidized in to the chlorides as shown by the following reaction.

$Cr + Cl_2 = CrCl_2$
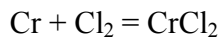
It should be noted that significant role was played by $CrCl_2$, $FeCl_2$ and $NiCl_2$ in propagating/promoting the corrosion process. The main reasons behind the faster formation of these chlorides were proposed on the basis of their molecular volume by Li and Spiegel [41]. Through XRD examination, it was found that $CrCl_2$ is not detected easily because $CrCl_2$ has large size molecular volume due to which its outward diffusion seems to be very slow. Another reason can be absence of porosity, due to which diffusion through scale is only possible by their ions rather than their molecules. Thus, $CrCl_2$ converts locally into its oxide form, neglecting its outward diffusion. At this instance, $CrCl_2$ in presence of higher oxygen potential, may form chromates and Cr_2O_3, due to concentration gradient. This reaction can be shown as:

$2CrCl_2 + 32O_2 = Cr_2O_3 + 2Cl_2$
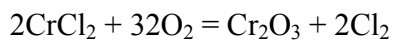
Few researchers have confirmed that solubility of Cr_2O_3 in NaCl-KCl melts is higher and tends to form chromates [40-46].

Cao and Norell [47, 48] investigated the effects of nitrogen uptake on 304L and 904L steel used in diesel exhaust systems, under humid air atmosphere at 450-600 °C, by

plasma nitriding. Plasma nitrided surface was found to be enhanced by N containing super-saturated expanded austenite (S-phase). Uptake of nitrogen was found to be more detrimental during oxidation of 304L and 904L because the oxide thickness of nitride was much higher than that on the nitride free 304L and 904L. It was due to decreasing activity of Cr on the nitrided layer, which had occurred due to strong bonding with N and obstructed the formation of protective oxides. This phenomenon was called short range ordering. For 904L, S-phase was found to be stable and improve its corrosion resistance. From their study it is clear that oxidation resistance of the as-received 904L can be high whereas enrichment of nitrogen can decrease its performance during service.

1.2.3 CYCLIC AND ISOTHERMAL EXPOSURES IN AIR

Oxidation and corrosion at higher temperatures above 500 °C play important role on performance of structural materials in industries such as power units, aerospace, gas turbines, heat treating systems and other metallurgical processing units. SASS grades often develop passive chromia layer at the initial stages when subjected to elevated temperatures, irrespective of partial pressure of oxygen. Prolonged periods of exposure at elevated temperatures may lead to detrimental effects on the passive layer. Thus, the feasibility of application of alloys depends over susceptibility of its resistance against oxidation/corrosion provided by protective scale. This property of scale ideally exhibits slow growth rate, good adherence, high stability and continuity, free from defects such as micro cracks or large voids. Minor alloying elements such as Mn, Ti, Si and Al can greatly influence the oxidation behavior. For example, oxides of Mn, Ti, Si and Al are

thermodynamically more unstable than that of Cr and have strong tendency to oxidize at the interface of environment and scale, which adversely affects the scale adhesion.

At higher temperatures, growth of scale is rapid in the initial stages due to which the rate of reaction is very slow and the corresponding thickness of the scale remains very thin. Movement of cations towards the scale becomes the rate controlling step which can be understood by scale thickening w.r.t time and follows parabolic rate law, under diffusion controlled kinetics, during isothermal/cyclic conditions. In general, the scale thickness depends on the time of exposure as given below

$$x = \sqrt{k_p t} \text{ ---1.1}$$

x= scale thickness; k_p= parabolic rate constant, t=time

The diffusion kinetics of any Fe-Ni-Cr alloy depends on Chromia scale because the critical chromium content offers adherence to the substrate. Selective oxidation of Cr by its removal from subsurface during oxidation/corrosion results in increase of the resistance of scale against cracking and spallation and also against the diffusion of other alloying elements such as Fe, Ni, Mo, Cu, Si through it. Another important parameter to determine the extent of oxidation/corrosion phenomenon depends on self diffusion coefficient and free energy formation of the reactive oxides. These two parameters are dependent on time, temperature and partial pressure of the environment.

Protective behavior of the scale exists for a finite period, up to breakdown of the scale under thermal cycling, due to lower coefficient of thermal expansion of the scale than that of the substrate. In an investigation, it was found that, thermal cycling promotes scale spallation whereas isothermal exposure can be more detrimental which may promote internal oxidation in addition to spallation. Most of the cases encounter particular

18

characteristics such as breakaway, pores, craters, etc which would have occurred due to segregation of oxide phases of the alloying elements over the junctions of grain boundaries. Further, the factors which affect the process of oxidation in the two different types of exposures are summarized below.

1. Kinetics

2. Types of stresses

3. Oxygen potential

4. Initial surface characteristics

1.2.3.1 KINETICS

The weight gain behavior under cyclic and isothermal exposures, depends on the nature of atmosphere and surface condition. In case of cyclic oxidation, the prime period of rapid growth of oxides is the initial time period of few hours and the secondary period consists of slow and steady growth with low rate of weight gain, with increasing temperature range. Whereas during isothermal exposure weight gain during the initial time periods may be low, at both the lower and higher temperatures. The degree of increase in weight gain in cyclic exposure is found to be much higher than the exposures from isothermal conditions. This profile remains common during most of the initial experimental conditions.

1.2.3.2 TYPES OF STRESSES

Comparison of the oxide scales formed during oxidation can be made from the change in the scale thickness. It depends on the stresses generated at different temperatures

and the nature of the substrate [49]. During oxidation, the inward and outward transfer of ions can dominate the surface by diffusion mechanism, which results due to stresses.

Huntz et. al. [50] suggested that NiO above 900 ˚C dominates the cationic diffusion over the scale due to which the scale grows at the outer interface. Whereas, Homma and Pyunn [51-54] performed test at 627 °C and proposed that NiO predominates the scale anionic diffusion due to which growth occurs at the inner interface. In case of Cr_2O_3 layer, Huntz et.al. [50] stated that the growth is promoted by cationic diffusion at the surface. Hussey, Lobnig, and Huntz [50, 51] proposed that oxygen and chromium have the diffusion coefficients in the same order of magnitude. Thus, oxygen can diffuse much faster than chromium and form massive oxides. Thus, at a lower range of temperature cationic diffusion seems to be prominent whereas at higher temperatures anionic diffusion occurs.

In order to get more insight of the mechanistic aspects of oxidation, several analytical techniques were used; particularly AES, SIMS, RHEED, laser Raman, Mössbauer, TEM and EELS [53]. Irrespective of exposure, either isothermal or cyclic oxidation, mixture of chromium oxide and iron oxide dominates the surface layer at a temperature range of 500 ˚C and above. During this initial stage, this layer grows mainly by outward diffusion of metal ions and resulted in weight gain. Investigations related to the growth of the oxide layer induced by stresses which may be created in three modes, (1) growth stresses; (2) thermal stresses; (3) relaxation.

In the case of cyclic oxidation, the nature of scale formed suffers from thermal stresses which may be due to cooling of the oxide scale to room temperature, resulting in

disturbances in diffusion phenomena during this process, compressive stresses are generated in the scale whereas tensile stresses are generated at the internal substrate.

These stresses can be closely related with the Pilling Bedworth ratio. Most authors have worked on Cr/Cr_2O_3, $NiCr/Cr_2O_3$ systems, which showed that growth of chromium oxide follows tensile as well as compressive stress behavior at the scale but the level of stresses is very small. It was observed by Daghigh et. al. [55, 56] that peaks for solid solution of NiCr grow more rapidly than Cr_2O_3 peaks at a higher temperature which can overlap the chromium peaks and introduce errors.

Thus, the outward growth of a scale takes place at a free surface with a minor amount of strains, followed by compression, whereas oxygen diffusion creates tensile strains in case of isothermal oxidation and the scale suffers from growth stresses. The nature of growth stress on the metal surface causes volume change of oxides resulting in recession at the oxide/metal interface.

At this stage the oxide scale exhibits intrinsic growth of new oxides leading to compressive stresses which often give rise to a situation called lateral growth of oxides. During the continuous exposures at a particular temperature and time this growth of oxide over the scale results in volume change and leads to compressive growth which may further result in spallation of scale.

1.2.3.3 RELAXATION

Relaxation is one of the most important parameters which occurs between the oxide and substrate. This period results in relief of the stresses which occur at the given scale growth at higher temperature. During cyclic exposure, the discontinuous time cycles result

in numerous changes in oxide morphology and thickness which results in non-uniform oxide growth. In the present situation, this non-uniform oxide growth from the SEM image can be observed by differences in the two zones, 1. Oxides formed by different geometries appearing in bright colors. 2. Visibility of surface which may be resulted due to incomplete oxidation.

In case of isothermal oxidation, continuous exposure led to formation of oxides in large volume than in cyclic oxidation. From the morphology, it is clear that the stresses induced by dense oxides are higher at the scale whereas the internal layer resulted in weakening from the base metal. The thickness of the oxide scale is more in isothermal exposure than that from cyclic exposure.

1.2.3.4 OXYGEN POTENTIAL

In view of the classical theory of oxidation proposed by Wagner [57, 58] which describes that the main diffusing element is a cation. By the outward diffusion of cation interface is created which results in vacancy/voids occupied by fresh metal at the interface region. The created vacancy is a major consideration in determining the kinetics and morphology of the oxide scale. During cyclic oxidation, occurrence of vacancies is more prominent at the surface because the potential of oxygen inside the furnace during the initial cycles is almost similar as of atmospheric oxygen. When the sample is exposed in air, shrinking of metal occurs at the scale which delays the growth of oxides, which decreases the rate of weight gain and thickness. At this stage vacancies created start condensing, into internal voids, without altering the external dimensions of the metal surface. These voids are occupied by oxygen. From increase in the number of cyclic exposures, the vacancies cause

non-uniform growth, due to which thin oxide scale is exhibited. Whereas in the isothermal oxidation, metal is covered with a uniform oxide scale, thus, the distribution of voids remains equally arranged. During short exposures, scale remains uniform, compact and columnar. Further, the number of voids formed is small and they rely on the metal-oxide interface. As oxidation time and temperature increase, the voids penetrate and combine with other voids across the metal. Thus, on longer oxidation times the potential of oxygen and its occupancy of voids into the interior of the metal increases resulting in decrease of the radius of the sample.

1.3. MOTIVATION

In waste to energy (WTE) power plants combustion of biomass reduces air pollution drastically but causes deposition of ash of complex chemistry on the boiler tubes. The oxidation and hot corrosion of tubes under such environment reduces the overall life of the material and sometimes results in serious plant accidents. 904L is one of the important materials in super austenitic steels family, which is not explored for its applications in such WTE boilers. Coal fired boiler tubes are usually operated between 550-700 ˚C or above, whereas biomass fired boilers are operated at lower temperature of 400-550 ˚C. It is therefore essential to understand the behavior of 904L SASS under complex salt mixtures of K, Na, Cl, and S for application at intermediate temperatures from 500-650 ˚C.

1.4 OBJECTIVES

The objectives of the present work are:

1. Study of cyclic and isothermal oxidation behavior of the super austenitic stainless steel 904L in air from 500 to 650 ˚C up to 100 h.

2. Study of the cyclic and isothermal hot corrosion behavior of the super austenitic stainless steel 904L in biomass ash environment of NaCl, KCl, Na_2SO_4 and K_2SO_4 with Cl:S of 40:60 (SM1) and 60:40 (SM2) from 500 to 650 ˚C up to 100 h.

3. Comparison of oxidation and hot corrosion behavior of 904L SASS under isothermal and cyclic conditions.

4. Flow chart on the experimental plan of work is shown in **Figure 1.1**.
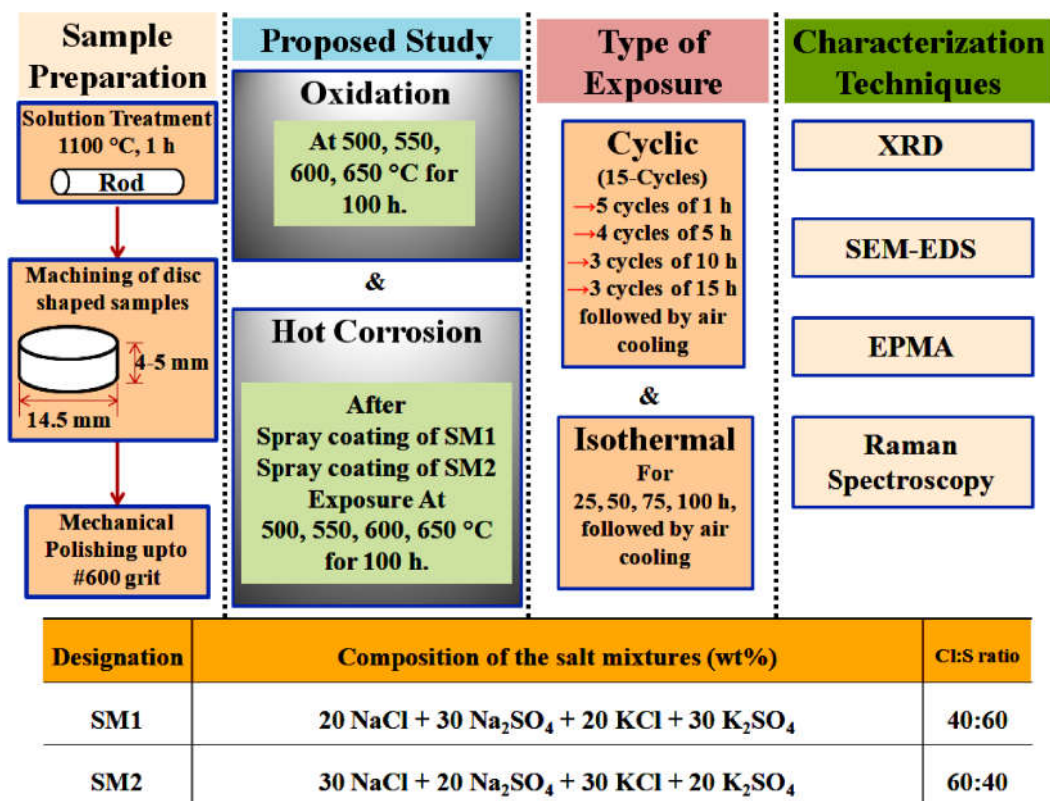
Figure 1.1: Flow chart of the plan of the experimental work.